

# Synthesis, In Vitro, and In Silico Evaluation of Organometallic Technetium and Rhenium Thymidine Complexes with Retained Substrate Activity toward Human Thymidine Kinase Type 1

Dominique Desbouis,<sup>†,‡,§</sup> Harriet Struthers,<sup>†,‡,§</sup> Vojtech Spiwok,<sup>||</sup> Tatiana Küster,<sup>§</sup> and Roger Schibli<sup>\*,‡,§</sup>

Department of Chemistry and Applied Biosciences, ETH Zurich, 8093 Zurich, Switzerland, Center for Radiopharmaceutical Science, ETH-PSI-USZ, Paul Scherrer Institute, 5232 Villigen PSI, Switzerland, Department of Structure and Function of Saccharides, Institute of Chemistry, Slovak Academy of Sciences, Dubravská Cesta 9, 84538 Bratislava, Slovak Republic

Received May 8, 2008

Human cytosolic thymidine kinase (hTK1) has proven to be a suitable target for noninvasive imaging of cancer cell proliferation using radiolabeled substrates such as [<sup>18</sup>F]fluorothymidine ([<sup>18</sup>F]FLT). However, a thymidine tracer useful for single photon emission tomography (SPECT) based on the inexpensive radionuclide technetium-99m would be of significant interest. In this work, a series of thymidine derivatives labeled with the organometallic [M(CO)<sub>3</sub>]<sup>+</sup> core (M = <sup>99m</sup>Tc, Re) were synthesized. Neutral, cationic, and anionic complexes were readily formed in aqueous media, and all were substrates of recombinant hTK1 when incubated with ATP. The neutral complexes were phosphorylated to a greater extent than the charged complexes. The extent of phosphorylation was further improved by increasing the spacer length separating thymidine and the organometallic core. A molecular dynamics simulation study performed with a modified hTK1 structure supported the experimental findings. In vitro cell internalization experiments performed in a human neuroblastoma cell line (SKNMC) showed low uptake of the charged complexes but significant uptake for the neutral, lipophilic complexes with a log *P* value > 1.

## Introduction

Human thymidine kinase 1 (hTK1<sup>a</sup>) is a cytosolic enzyme that catalyzes the Mg<sup>2+</sup>-dependent  $\gamma$ -phosphate transfer from ATP to the 5'-hydroxyl group of thymidine (dT), resulting in the formation of thymidine 5'-monophosphate (dTMP).<sup>1</sup> hTK1 activity is known to fluctuate during the cell cycle.<sup>2</sup> It has been reported that high levels of hTK1 are observed during the S-phase of the cell cycle, as well as in a number of rapidly proliferating and malignant cells, where hTK1 expression is increased up to 15-fold with respect to normal cells.<sup>3–7</sup> Thus, hTK1 has been identified as a suitable target for noninvasive imaging and therapy of malignant cells using nonradioactive and radioactively labeled dT and uridine (dU) derivatives.

An important feature of nucleoside metabolism is the rapid intracellular phosphorylation of nucleosides to nucleotides, which renders them unable to penetrate biological membranes and thus results in the "trapping" of nucleotides inside cells. In the case of radioactively labeled thymidine (or other

nucleoside) analogues, this phenomenon leads to amplification of the radioactive signal and facilitates the detection of proliferation sites. Thymidine and thymidine analogues labeled with PET radionuclides, such as <sup>11</sup>C-methyl-thymidine, <sup>76</sup>Br-fluoro-deoxyuridine (<sup>76</sup>Br-BFU), and <sup>18</sup>F-fluoro-deoxythymidine (<sup>18</sup>F-FLT), are either under development or already in use as proliferation markers.<sup>8,9</sup> However, the complexity of PET chemistry, the high costs of PET isotope production, and the very short half-lives of PET isotopes are considerable drawbacks. In contrast, the radionuclide <sup>99m</sup>Tc, useful for single photon emission tomography (SPECT), is readily available at low cost and has very favorable decay properties ( $\gamma$ -emission, 140 keV, *t*<sub>1/2</sub> = 6.0 h). Similarly, <sup>186</sup>Re and <sup>188</sup>Re, two isotopes of technetium's higher homologue rhenium, are among the most promising radionuclides for therapeutic applications. It is therefore of interest to develop <sup>99m</sup>Tc- and \*Re-radiolabeled substrates, which target hTK1, for both diagnostic and therapeutic applications.

The group of Tjarks has published a number of dT derivatives functionalized at position N3 with *closo-o*-carboranes, which maintain the important substrate activity toward hTK1.<sup>10–15</sup> Therefore, it is surprising that attempts to develop radiometal labeled thymidine complexes, functionalized at position N3 with, e.g., a DOTA chelator and radiolabeled with <sup>68</sup>Ga and <sup>111</sup>In, capable of being phosphorylated by hTK1, have been unsuccessful.<sup>16</sup> Celen et al. have more recently evaluated a <sup>99m</sup>Tc<sup>V</sup>-MAMA-propyl-thymidine complex as a potential probe for in vivo visualization of tumor cell proliferation with SPECT. However, they found that the corresponding ligand (and presumably also the <sup>99m</sup>Tc-complex) could not be phosphorylated because it is too bulky.<sup>17</sup> Our group has focused on the development of tumor targeting biomolecules labeled with the water-soluble and water-stable organometallic precursor [M(H<sub>2</sub>O)<sub>3</sub>(CO)<sub>3</sub>]<sup>+</sup> (M = <sup>99m</sup>Tc, Re).<sup>18,19</sup> *fac*-[M(CO)<sub>3</sub>]<sup>+</sup> complexes can be designed so that they are sterically less demanding

\* To whom correspondence should be addressed. Phone: +41 (0)56 310 2837. Fax: +41 (0)56 310 2849. E-mail: roger.schibli@psi.ch.

<sup>†</sup> both authors contributed equally to this work.

<sup>‡</sup> Department of Chemistry and Applied Biosciences, ETH Zurich.

<sup>§</sup> Center for Radiopharmaceutical Science, ETH-PSI-USZ, Paul Scherrer Institute.

<sup>||</sup> Department of Structure and Function of Saccharides, Institute of Chemistry, Slovak Academy of Sciences.

<sup>a</sup> Abbreviations: hTK1, human thymidine kinase 1; ATP, adenosine triphosphate; dT, thymidine; dTMP, thymidine 5'-monophosphate; dU, uridine; PET, positron emission tomography; <sup>76</sup>Br-BFU, <sup>76</sup>Br-fluoro-deoxyuridine; <sup>18</sup>F-FLT, <sup>18</sup>F-fluoro-deoxythymidine; SPECT, single photon emission tomography; DOTA, 1,4,7,10-tetraazacyclododecane-*N,N',N'',N'''*-tetraacetic acid; MAMA, monoamino-monoamide dithiol; Cys, cysteine; DETA, diethylene triamine; IDA, imino diacetic acid; ADP, adenosine diphosphate; NADH, reduced nicotinamide adenine dinucleotide; PK, pyruvate kinase; LDH, lactate dehydrogenase; DTT, dithiothreitol; PEP, phospho(enol)pyruvate; PBS, phosphate buffered saline; MD, molecular dynamics; rmsd, root-mean-square deviation; dTTP, thymidine 5'-triphosphate; bTK, bacterial thymidine kinase; TEAP, triethylammonium phosphate.

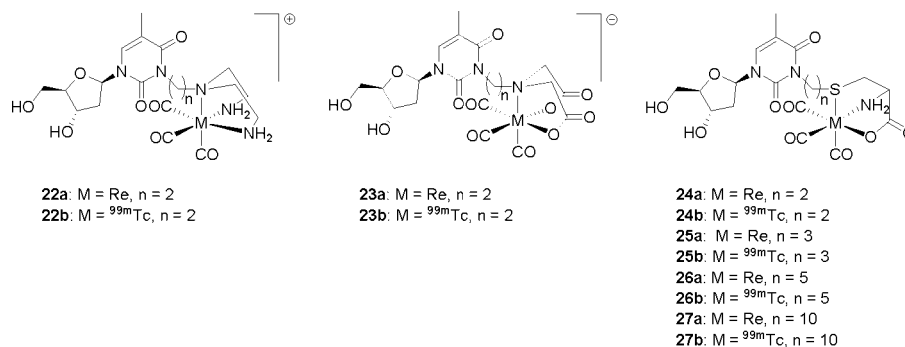


**Figure 1.** Library of Re and <sup>99m</sup>Tc complexes of thymidine developed in this study.

than, e.g., octahedral or square-pyramidal complexes of technetium and rhenium in high oxidation states ( $>+I$ )<sup>20</sup> or (radio)metal complexes of, e.g., DOTA-type chelators. Thus, it was hypothesized that N3-functionalized dT derivatives labeled with the  $[M(CO)_3]^+$  core are likely to be suitable substrates for hTK1.

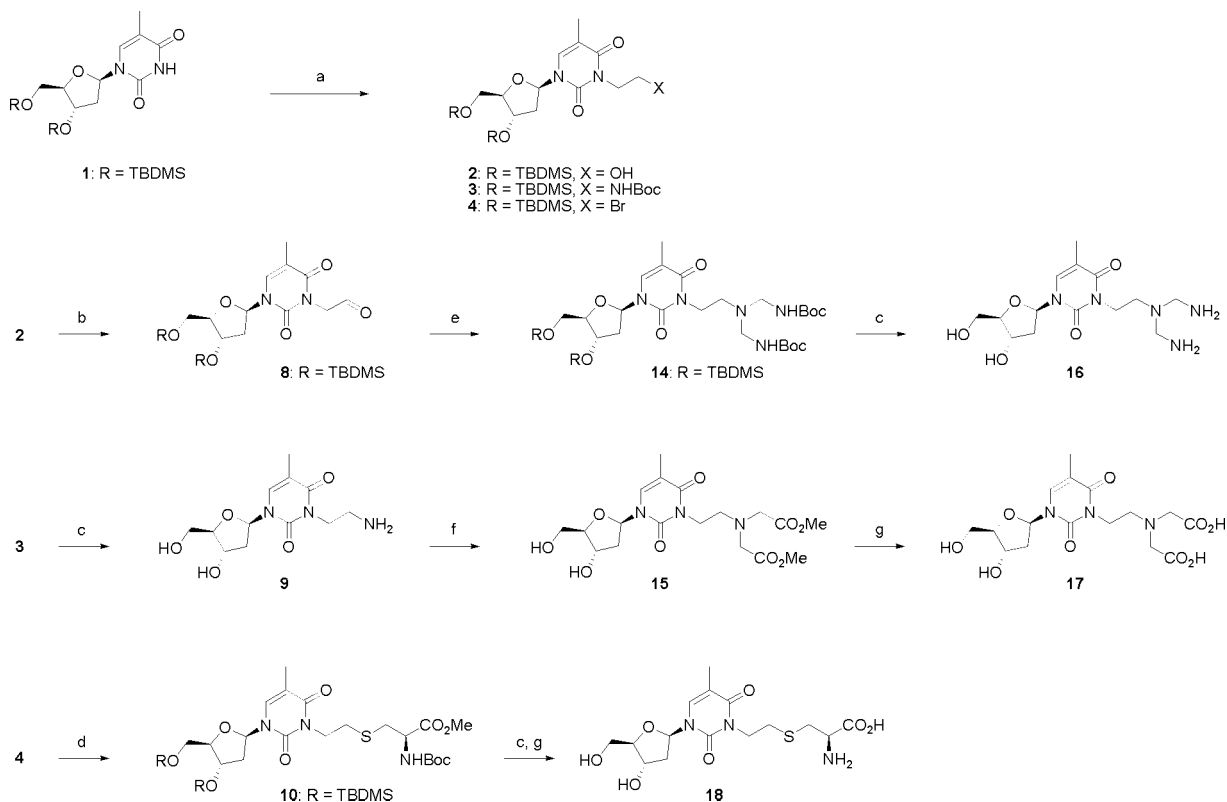
In this work, we describe the synthesis and systematic *in vitro* characterization of a series of novel N3-functionalized organometallic thymidine analogues (Figure 1). In the first series of compounds, the influence of the overall charge of the thymidine complex on substrate activity was investigated. In the second series of thymidine derivatives, the length of the spacer connecting the thymine base and the distal metal complex was varied. The phosphorylation of the <sup>99m</sup>Tc and Re complexes in the presence of hTK1 and ATP was assessed quantitatively relative to thymidine. Molecular dynamics simulations provided further insight into the binding orientation of these compounds in the active site of the enzyme as well as the experimentally observed trends in substrate activity of the novel complexes. *log P* values and the cell internalization capacity of the radioactive complexes in human neuroblastoma SKNMC cells were also assessed.

## Results and Discussion

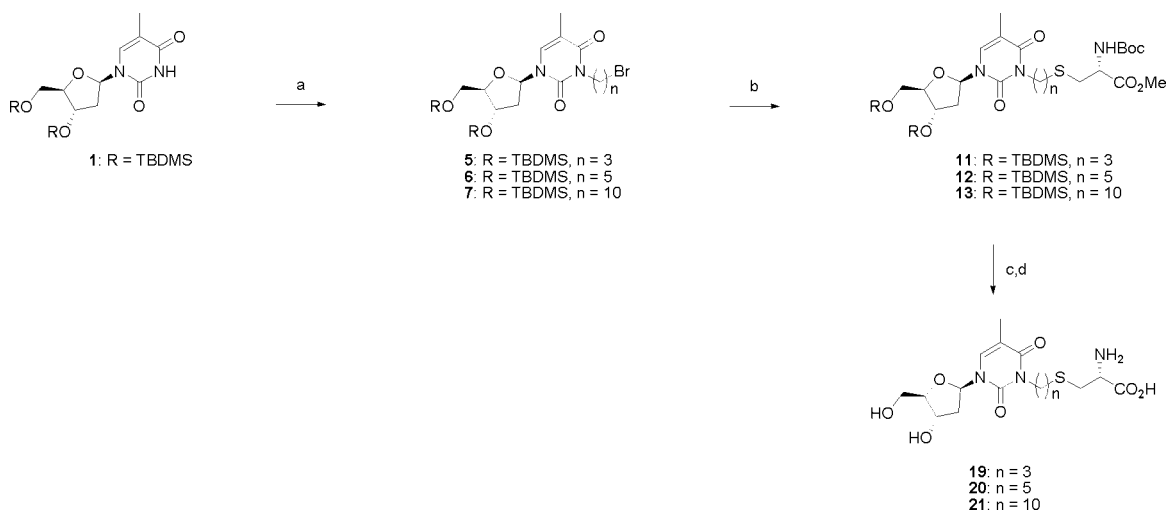
Our group has previously reported the synthesis and characterization of a series of thymidine derivatives functionalized at the C5' position and labeled with the organometallic  $[M(CO)_3]^+$  core (M = <sup>99m</sup>Tc, Re).<sup>21–23</sup> These complexes inhibit hTK1, but functionalization at position C5' prevents phosphorylation. The complexes are therefore unattractive as potential radiotracers for noninvasive imaging of tumor progression because the mechanism by which they would be trapped inside cancer cells relies on phosphorylation of the complex. With this in mind, we set out to develop new technetium and rhenium labeled thymidine complexes, which are still recognized as substrates by hTK1. There are several sites of thymidine, such as C3', N3, and C5, which could be modified with a radiometal complex while leaving the C5' position unmodified and potentially able to be phosphorylated. Of the positions mentioned, C5 is least attractive because of the low steric tolerance of hTK1 at this position as compared, e.g., to HSV1 TK.<sup>24–26</sup> In light of the pioneering work of the Tjarks group on N3-substituted carborane thymidines,<sup>10–12,14,27–29</sup> we considered the N3 position most appealing for functionalization and labeling with the  $[M(CO)_3]^+$  core (M = <sup>99m</sup>Tc, Re). We have already reported the qualitative assessment of a small series of N3-substituted, organometallic thymidine derivatives as substrates for hTK1 from a separate recent study.<sup>30</sup> These data encouraged us to perform a more systematic investigation.

## Chemistry

**Ligand Synthesis.** From previous studies by our group and others, we have learned that tridentate poly-amino, polycarboxylic acid, and amino acid based ligand systems form very stable and kinetically inert complexes with the organometallic  $[M(CO)_3]^+$  core with favorable pharmacologic properties.<sup>20,31–35</sup> This knowledge, and the fact that the overall charge of the complex could have a decisive influence on the substrate activity of corresponding thymidine derivative, prompted us to introduce three different chelating systems (cysteine, Cys; diethylene triamine, DETA; imino diacetic acid, IDA) at position N3 of thymidine, which give rise to neutral, positively, and negatively charged complexes when reacted with the  $[M(CO)_3]^+$  core. In the first series of compounds, the chelating systems were separated from the thymidine part of the molecule by an ethyl spacer. The syntheses of compounds **16**, **17**, and **18** are outlined in Scheme 1. Thymidine derivatives **2–4** were synthesized from 3',5'-bis-*O*-(*tert*-butyldimethylsilyl)thymidine,<sup>36</sup> **1**, which was reacted with either excess 2-bromoethanol, *N*-Boc-aminobromoethane, or 1,2-dibromoethane in dry DMF in the presence of cesium carbonate for 4 h. The crude reaction mixtures were purified by column chromatography to give 3-(2-hydroxyethyl)-3',5'-bis-*O*-(*tert*-butyldimethylsilyl)thymidine, **2**, in 91% yield, 3-(2-*N*-Boc-aminoethyl)-3',5'-bis-*O*-(*tert*-butyldimethylsilyl)thymidine, **3**, in 97% yield, and 3-(2-bromoethyl)-3',5'-bis-*O*-(*tert*-butyldimethylsilyl)thymidine, **4**, in 95% yield. 3-(2-Hydroxyethyl)-3',5'-bis-*O*-(*tert*-butyldimethylsilyl)thymidine, **2**, was oxidized with Dess–Martin periodinane to the corresponding aldehyde 3-(2-acetyl)-3',5'-bis-*O*-(*tert*-butyldimethylsilyl)thymidine, **8**, in 90% yield. The DETA chelating system was introduced by the reductive amination of **8** with *N,N'*-bis(Boc)diethylenetriamine in MeOH. The Boc and silyl groups of the protected intermediate **14** were removed in methanolic HCl to give **16** in 57% yield. Similarly, the Boc and silyl protecting groups of 3-(2-*N*-Boc-aminoethyl)-3',5'-bis-*O*-(*tert*-butyldimethylsilyl)thymidine, **3**, were removed in methanolic HCl to give 3-(2-aminoethyl)thymidine, **9**, in 81% yield. The IDA chelating system was introduced by reaction of **9** with three equivalents of methyl bromoacetate and three equivalents of triethylamine in MeCN to give the protected intermediate **15** in 63% yield. The methyl esters were removed by saponification in an NaOH solution to afford ligand **17**. The Cys chelating system was introduced via the reaction of 3-(2-bromoethyl)-3',5'-bis-*O*-(*tert*-butyldimethylsilyl)thymidine, **4**, with commercial *N*-Boc-L-cysteine methyl ester and cesium carbonate in dry DMF to give **10** (85%). The Boc and silyl protecting groups were removed by stirring in methanolic HCl for 4 h, and the methyl ester was hydrolyzed by increasing the

**Scheme 1.** Synthesis of Thymidine Derivatives with an Ethyl Spacer, Leading to  $M(\text{CO})_3$  Complexes of Varied Overall Charge<sup>a</sup>

<sup>a</sup> (a)  $\text{BrCH}_2\text{CH}_2\text{X}$ ,  $\text{Cs}_2\text{CO}_3$ , DMF; (b) Dess–Martin periodinane,  $\text{CH}_2\text{Cl}_2$ ; (c) HCl, MeOH; (d)  $\text{HSCH}_2\text{CH}(\text{CO}_2\text{Me})\text{NHBoc}$ ,  $\text{Cs}_2\text{CO}_3$ , DMF; (e)  $\text{NH}(\text{CH}_2\text{CH}_2\text{NHBoc})_2$ ,  $\text{NaBH}_3\text{CN}$ , MeOH; (f)  $\text{BrCH}_2\text{CO}_2\text{Me}$ , TEA, MeCN; (g) NaOH,  $\text{H}_2\text{O}$ .

**Scheme 2.** Synthesis of Thymidine Derivatives with Increasing Spacer Length between the Nucleoside and the Metal Chelating System<sup>a</sup>

<sup>a</sup> (a)  $\text{Br}(\text{CH}_2)_n\text{Br}$ ,  $\text{Cs}_2\text{CO}_3$ , DMF; (b)  $\text{HSCH}_2\text{CH}(\text{CO}_2\text{Me})\text{NHBoc}$ ,  $\text{Cs}_2\text{CO}_3$ , DMF; (c) HCl, MeOH; (d) NaOH,  $\text{H}_2\text{O}$ .

pH with 5 M NaOH. The solution was neutralized before purification by solid phase extraction to yield ligand **18** (62%).

To investigate the influence of the spacer length between thymidine and the cysteine chelating system, we prepared compounds **19**, **20**, and **21** (Scheme 2) according to the same procedure as compound **18**. 3',5'-bis-*O*-(*tert*-butyldimethylsilyl)thymidine, **1**, was reacted with the appropriate dibromoalkane to form the intermediates **5**, **6**, and **7** upon nucleophilic substitution (Scheme 2). The yields were 62%, 81%, and 82%, respectively. Intermediates **11** (100%), **12** (78%), and **13** (93%) were synthesized by reaction with *N*-Boc-*L*-cysteine methyl ester

according to the procedure outlined above for compound **10**. Deprotection of the Boc and silyl groups was performed in methanolic HCl. The methyl esters were then hydrolyzed by increasing the pH with 5 M NaOH to give the free ligands **19** (78%), **20** (80%), and **21** (78%).

**Syntheses of Organometallic Thymidine Complexes 22–27.** The organorhenium complexes **22a–27a** were prepared from the precursor  $[\text{ReBr}_3(\text{CO})_3][\text{NEt}_4]_2$  and a stoichiometric amount of the corresponding ligand in a mixture of MeOH and water at 50 °C. In each case, the quantitative formation of the product was observed by HPLC. The crude products

were purified by solid phase extraction using SepPak columns and a water–MeOH gradient. The IR spectra of all of the rhenium complexes revealed the typical *fac*-Re(CO)<sub>3</sub> pattern with significantly blue-shifted, intense CO stretching frequencies (around 2020 and 1880 cm<sup>-1</sup>) compared to the starting material [ReBr<sub>3</sub>(CO)<sub>3</sub>]<sup>2-</sup> (2000 and 1868 cm<sup>-1</sup>). NMR spectroscopic analyses provided strong evidence that the metal core is site-specifically coordinated via the tridentate metal chelating systems introduced at position N3. The proton NMR spectra showed significant, low field shifts of the Cys, DETA, and IDA protons after metal chelation. The protons in the  $\alpha$ - and  $\beta$ -positions of the cysteine chelate gave very broad signals after Re(CO)<sub>3</sub> coordination. This has been observed in other organometallic technetium and rhenium complexes containing thioethers.<sup>34,37</sup> In addition, the coupling patterns of these protons were characteristic for a tridentate  $\kappa N, \kappa N, \kappa N$ - (in the case of the DETA chelator), a  $\kappa O, \kappa N, \kappa O$ - (in the case of the IDA chelator), and a  $\kappa N, \kappa S, \kappa O$ - coordination (in the case of the Cys chelating system) of the M(CO)<sub>3</sub> core. The patterns were in agreement with similar examples reported in the literature.<sup>21,32,34</sup> The organometallic complexes **22a–24a** were readily soluble in water. For in vitro experiments complexes **25a–27a** were dissolved by addition of a small amount of DMSO (5% of the total volume).

The corresponding radioactive technetium-99m complexes **22b–27b** were prepared quantitatively after 45 min at 95 °C in physiological phosphate buffer (PBS; pH = 7.4) using the organometallic precursor [<sup>99m</sup>Tc(H<sub>2</sub>O)<sub>3</sub>(CO)<sub>3</sub>]<sup>+</sup> (IsoLink).<sup>18</sup> A single species was formed with all of the nucleoside derivatives. Characterization of the radioactive complexes **22b–27b** was accomplished by comparison of the retention times observed in the  $\gamma$ -HPLC trace with those in the UV-trace of the corresponding rhenium complexes **22a–27a**, a procedure which is common in radiopharmacy (see, e.g., complexes **24a/b** in Figure 2A,B). The retention times matched for all pairs of complexes within the experimental limitations. The stability of the complexes was evaluated in PBS buffer at 37 °C for 24 h. Decomposition or reoxidation of the complexes to either [<sup>99m</sup>TcO<sub>4</sub>]<sup>-</sup> or other side products was minor (<5%). This is an acceptable stability for Tc-99m radiopharmaceuticals to be applied in vivo. For in vitro studies, the <sup>99m</sup>Tc-complexes were separated from the unreacted thymidine derivatives **16–21** via HPLC.

### In Vitro Evaluation of the Organometallic Thymidine Complexes

**Phosphorylation Assay.** The hTK1 substrate activities of all target rhenium complexes were assessed using a coupled thymidine kinase–pyruvate kinase–lactate dehydrogenase UV assay ( $\lambda = 340$  nm) as previously described.<sup>27,38</sup> The results are presented in Table 1. For our studies, the phosphorylation of thymidine was arbitrarily set as 100%. The compound 3-(2-propyn-1-yl)thymidine, a known N3-functionalized substrate of hTK1, was also included in this assay, both for comparison and as a control. We found for this specific compound a phosphorylation of  $86.7 \pm 2.2\%$ , which is slightly lower than previously published results ( $102.1 \pm 3.6\%$ ), presumably due to differences in the experimental setup.<sup>28</sup> In the first series of compounds with different overall charges but a constant spacer length (an ethyl spacer between thymidine and the organometallic complex), the neutral complex was most readily phosphorylated ( $46.2 \pm 3.6\%$ ). The anionic complex **24a** revealed a phosphorylation rate of  $33.8 \pm 2.4\%$ . The lowest phosphorylation was

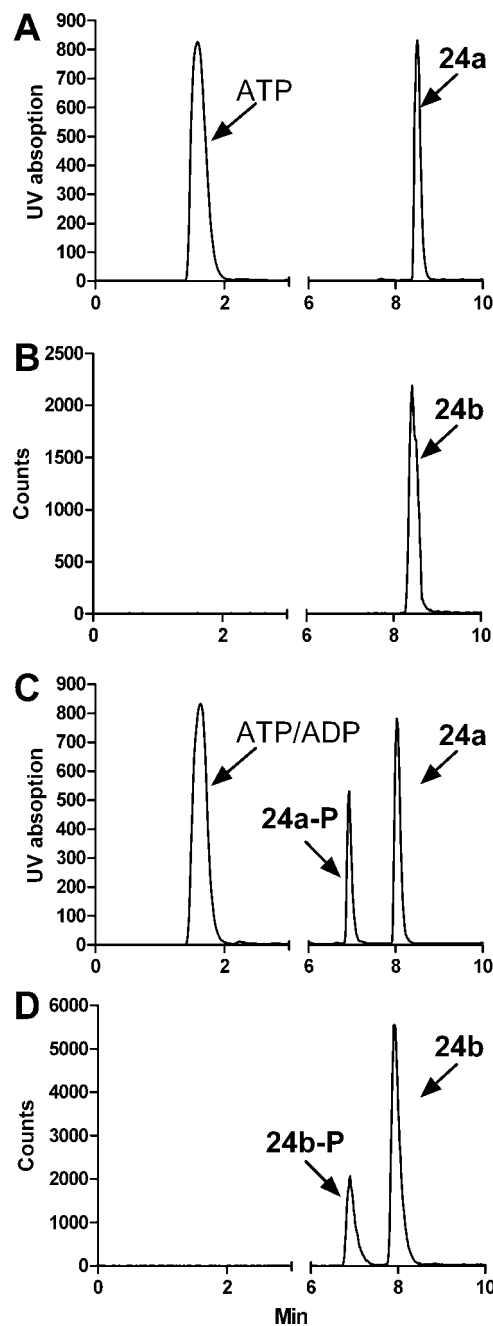


**Figure 2.** (A) UV-HPLC trace of rhenium complex **24a** and ATP before addition of hTK1. (B)  $\gamma$ -HPLC trace of <sup>99m</sup>Tc-complex **24b** and ATP before addition of hTK1. (C) UV-HPLC trace of rhenium complex **24a** and ATP after incubation with hTK1 for 1 h at 37 °C. (D)  $\gamma$ -HPLC trace of <sup>99m</sup>Tc-complex **24b** and ATP after incubation with hTK1 for 1 h at 37 °C.

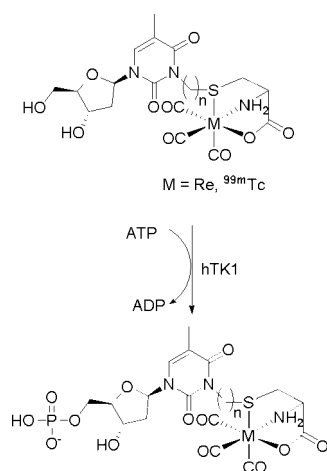
observed for the cationic complex **22a** ( $16.4 \pm 0.7\%$  compared to thymidine). This trend is in agreement with the qualitative results of a previous study of N3-functionalized thymidine Tc-99m complexes.<sup>30</sup> Thus, the overall charge of the thymidine complexes appears to have a significant influence on their substrate activity, with neutral complexes appearing to be most favorable. The fact that the positive charge has a deleterious effect was surprising given that Byun et al. have shown that zwitterionic NH<sub>3</sub><sup>+</sup>-*nido-m*-carborane-substituted thymidine analogues (with a propyl spacer) showed high substrate activity.<sup>28</sup> However, several other parameters (e.g., log *P* values, solubility etc.) should be considered before drawing meaningful conclusions, for which a side-by-side comparison of organometallic

**Table 1.** Phosphorylation of Complexes **22a–27a** and the Known N3 Functionalized Substrate 3-(2-Propyn-1-yl)thymidine

compound	phosphorylation relative to dT [%] <sup>a</sup>
<b>22a</b>	16.4 ± 0.7
<b>23a</b>	33.8 ± 2.4
<b>24a</b>	46.2 ± 3.6
<b>25a</b>	46.9 ± 2.6
<b>26a</b>	57.5 ± 2.2
<b>27a</b>	71.5 ± 4.7
3-(2-propyn-1-yl)thymidine	86.7 ± 2.2
dT	100 <sup>b</sup>

<sup>a</sup> Mean ± SD values are based on three experiments per compound. <sup>b</sup> The phosphorylation of dT was arbitrarily set to 100%.

### Scheme 3. Phosphorylation of Complexes **24–27** by hTK1 in the Presence of ATP



and carborane dT-derivatives would be necessary. For our own further studies, neutral complexes in which the organometallic complex is incorporated via the Cys chelating system were synthesized to investigate the influence of the spacer length on the substrate activity. Complexes **25a**, **26a**, and **27a** show phosphorylation relative to thymidine of 46.9 ± 2.6%, 57.5 ± 2.2%, and 71.5 ± 4.7%, respectively. These results suggest a direct correlation between tether length and substrate activity. It is noteworthy that the metal free ligands **18**, **20**, and **21** are recognized as substrates of hTK1 and they revealed a similar trend with respect to substrate activity: (**18** < **20** < **21**; data not shown).

In a second, direct assay, the radioactive and nonradioactive complexes **22–27** were incubated with ATP and recombinant hTK1 only (Scheme 3). The enzymatic reactions were analyzed by HPLC (UV-trace at  $\lambda = 254$  nm for the rhenium complexes,  $\gamma$ -trace in the case of the radioactive Tc-<sup>99m</sup> complexes). For both the <sup>99m</sup>Tc and the Re compounds, phosphorylation resulted in a measurable shift in retention time on a C<sub>18</sub> reversed phase column (Figure 2). This enabled the unambiguous distinction of the monophosphorylated products **22-P–27-P** from the starting material. In the cases of complexes **24a** and **26a**, we were able to obtain the mass peaks of **24a-P** and **26a-P** ( $m/z = 739.8$ , [M]H<sup>+</sup>;  $m/z = 782.1$ , [M]H<sup>+</sup>) after HPLC purification of the reaction mixtures (see Supporting Information). In time dependent, HPLC experiments of complex **23a**, an increase in the concentration of the monophosphorylated species **23a-P** and corresponding decrease in the concentration of the starting complex was observed (see Supporting Information). After 2 h incubation at 37 °C, approximately 50% of the complex **23a** had been phosphorylated.

**Table 2.** log *P* Values of Complexes **22b–27b** and Internalization into SKNMC Cells

compound	log <i>P</i>	% ID/(mg/mL) <sup>a</sup>
<b>22b</b>	-1.67 ± 0.02	
<b>23b</b>	-1.08 ± 0.06	0.6 ± 0.1
<b>24b</b>	-0.42 ± 0.01	
<b>25b</b>	-0.31 ± 0.00	
<b>26b</b>	0.42 ± 0.00	1.2 ± 0.1
<b>27b</b>	1.11 ± 0.08	4.8 ± 0.5
<sup>3</sup> H-dT		29.0 ± 3.5

<sup>a</sup> 120 min after incubation.

**Cell Internalization Experiments.** hTK1 is located in the cytosol, and therefore a potential substrate has to pass through the cell membrane before it can be phosphorylated. If this transport is not achieved actively via nucleoside transporters, then it must occur by passive diffusion. This has been suggested as the major cell internalization route for the carborane-thymidine derivatives reported by Tjarks et al.<sup>28</sup> One of the decisive parameters in the ability of a compound to penetrate cells via passive diffusion is lipophilicity, which can be evaluated using the *n*-octanol/water partition coefficient (log *P*). The log *P* values of compounds **22b–27b** were determined radiometrically.<sup>39</sup> The results are presented in Table 2. Complexes **22b–24b** with ethyl spacers all exhibited negative log *P* values ranging from -1.672 ± 0.017 to -0.417 ± 0.005. The values indicate that these complexes with a short spacer are hydrophilic and are therefore unlikely to be able to enter the cells via passive diffusion. As expected in this series, the neutral complex was the least hydrophilic. The lipophilicity of the compounds increased with the successive elongation of the spacer entity. Compounds **26b** (C<sub>5</sub> spacer) and **27b** (C<sub>10</sub> spacer) exhibit positive log *P* values of 0.424 ± 0.003 and 1.108 ± 0.080, respectively. Further in vitro cell experiments were performed with compounds **24b** (log *P* = -1.08 ± 0.06), **26b** (log *P* = 0.424 ± 0.00), and **27b** (log *P* = 1.11 ± 0.08). **24b** displayed a low uptake in SKNMC cells of 0.6 ± 0.1% ID/(mg/mL), which is not surprising given the hydrophilic nature of this complex. However, complex **26b**, which has a positive log *P* value, also displayed a very low uptake with 1.2 ± 0.1% ID/(mg/mL) after 2 h incubation time. Complex **27b** revealed a significantly higher uptake in SKNMC cells, with up to 4.8 ± 0.5% ID/(mg/mL). For comparison, the natural substrate for hTK1, <sup>3</sup>H-dT, which is internalized into cancer cells by facilitated transport, had a total uptake of approximately 30% ID/(mg/mL) under the same conditions.

### Computational Studies

Several crystal structures of hTK1 have been published in the past few years (e.g., PDB code 1XBT and 1W4R).<sup>24,25</sup> In these structures, hTK1 hosts the feedback inhibitor thymidine 5'-triphosphate (dTTP) in its phosphate acceptor site and consists of two domains, an  $\alpha/\beta$ -domain and a small zinc containing lasso-domain. The active site is situated between the  $\alpha/\beta$ -domain and the lasso-domain. The small domain (Cys153-Asn234) contains a long, flexible lasso-shaped loop, which upon substrate binding undergoes a large conformational change. More recently, the structures of several bacterial TKs have become available, namely those of *Clostridium acetobutylicum* TK (PDB code 1XX6),<sup>40</sup> *Bacillus cereus* TK (PDB code 2J9R),<sup>41</sup> and *Thermotoga maritima*.<sup>42</sup> The bacterial TKs have similar structures to hTK1 but feature a more open lasso loop. While the structures of hTK1 represent “closed” forms of the enzyme, the bTKs display more “open” or “semi-open” structures in the holo form. This slight structural difference was crucial for our in silico

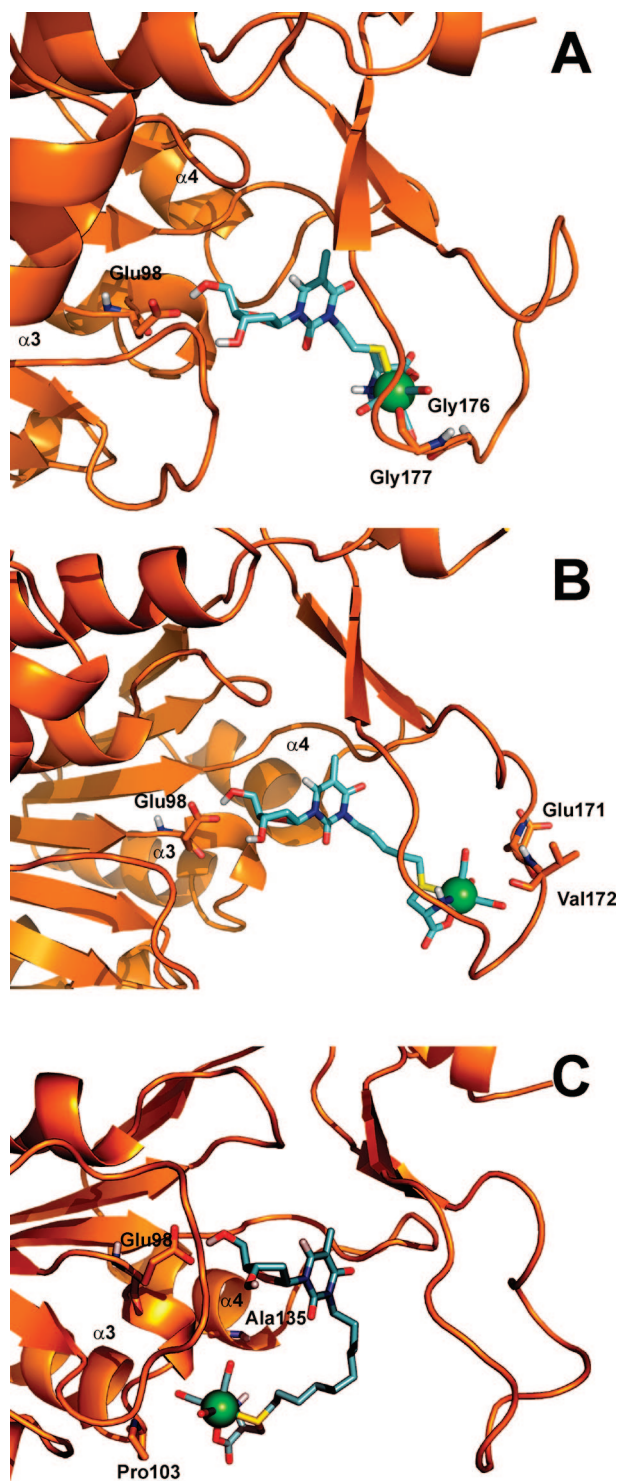


**Figure 3.** Minimized average position of thymidine derivatives in the active site over the last 200 ps of the MD run. (A) **24a**, (B) **26a**, (C) **27a**.

studies with complexes **24a**, **26a**, and **27a** because the close contact between the lasso loop of the zinc domain and position N3 of dTTP (forming a hydrogen bond between N3 of and the carbonyl oxygen of Val172) prevented direct “docking” of our N3-functionalized thymidine analogues into the active site of hTK1. A homology model of hTK1 with a “semi-open” conformation of the lasso loop was constructed by adopting the lasso loop from *Clostridium acetobutylicum* thymidine kinase. A very similar approach was successfully proposed and published by Byun et al.<sup>27</sup> We hypothesized that binding of the

complexes in the active site of the homology model results in a partial closing of the lasso loop, leading to an orientation of the ribose, which makes it amenable to the transfer of the  $\gamma$ -phosphate group of ATP. Alignment of *B. cereus* TK, hTK1, and our modified hTK1 structure revealed close structural resemblance but significant differences in the lasso loop region (see Figures A6 and A9 in the Supporting Information). The model was carefully validated with and without the natural substrate dT using MD simulations and assessing the rmsd from the initial structure. The rmsd of the homology model was stable and reached a plateau between 0.350 and 0.400 nm after 600 ps (Figure A7 and A8 in the Supporting Information). Thus, the model used for these studies appeared suitable for the subsequent MD simulations.

The rmsd of compounds **24a**, **26a**, and **27a** fluctuated, especially in the case of complex **27a**, which possesses a long and flexible spacer (Figure A10 in the Supporting Information). However, the calculations revealed in all cases that the thymine ring as well as the ribose occupied the thymidine-binding site in the proposed, regular orientation. Thus, the position of the base and ribose did not seem to be affected by substitution at position N3. The hydrogen-bond interaction between the 5'-oxygen and Glu98 (important for the deprotonation of O5' necessary for phosphorylation) was conserved for all complexes over the course of all the MD simulations (Figure 3). These observations are in agreement with the fact that all complexes are reasonably good substrates of hTK1. The bulky organometallic moieties of complexes **24a** and **26a** are oriented toward the “open” lasso loop, minimizing steric hindrance. In addition, we observed a number of additional contacts between the protein and the thymidine complexes (see Figure A11 in the Supporting Information). The organometallic cores of both complexes **24a** and **26a** showed contacts with the lasso loop. **24a** displayed contacts with the two consecutive glycine residues 176 and 177, while **26a** had contacts with Glu171 and Val172. The organometallic moiety of complex **27a** is relocated toward the surface of the enzyme due to the increased flexibility of the longer spacer. It revealed contacts between helix  $\alpha$ 3a (via Pro103) and helix  $\alpha$ 4 (via Ala135).

## Conclusion

A set of six neutral, anionic, and cationic organometallic rhenium and technetium complexes of thymidine have been successfully synthesized and characterized. Systematic in vitro experiments have proven for the first time that thymidine derivatives functionalized with a transition metal complex at position N3 of the nucleobase are recognized as substrates by recombinant hTK1. It could be demonstrated that neutral and anionic complexes are more readily accepted as substrates than cationic complexes. Furthermore, in the case of the neutral rhenium complexes, affinity for hTK1 increases as the length of the spacer separating thymidine and the organometallic core increases. An in silico molecular dynamics simulation study based on a homology model of hTK1 with a modified lasso loop region was successfully performed. The data confirmed that our thymidine complexes could be accommodated in the active site of hTK1 and that the partial closure of the lasso loop upon substrate binding, which is necessary for phosphorylation, is possible. The modeling suggested that the flexibility of a longer spacer between the thymidine and organometallic core further improves the ability of the complexes to be accommodated in the binding site, which is in agreement with the experimental findings. In vitro cell experiments performed with radioactive technetium-99m homologues showed superior cell

membrane permeability for the complexes with a log *P* value > 1. These encouraging results warrant further in vitro and in vivo investigations of the organometallic thymidine complexes to fully elucidate their radiodiagnostic and therapeutic potential. Corresponding experiments are ongoing in our laboratories.

## Experimental Section

**General.** All chemicals were purchased from Sigma-Aldrich or Fluka, Buchs, Switzerland. All chemicals and solvents were of reagent grade and were used without further purification unless otherwise stated.  $[\text{Na}][^{99\text{m}}\text{TcO}_4]$  was eluted from a  $^{99}\text{Mo}/^{99\text{m}}\text{Tc}$ -generator (Mallinckrodt-Tyco, Petten, The Netherlands) with a 0.9% saline solution. The precursors *fac*- $[\text{Re}(\text{CO})_3(\text{H}_2\text{O})_3]^+$  and *fac*- $[\text{Re}(\text{CO})_3\text{Br}_3][\text{NET}_4]_2$  were prepared according to published procedures.<sup>18,43</sup> Experimental procedures for the synthesis of compounds **16**, **17**, and **19** can be found in the Supporting Information. Reactions were monitored by HPLC or by thin layer chromatography (TLC) using precoated silica gel 60  $F_{254}$  aluminum sheets (Merck) and visualized by UV absorption or stained with a solution of ninhydrin in EtOH. Column chromatography was performed using silica gel 60 (Fluka; particle size 0.04–0.063 mm). HPLC analyses were performed using a Merck-Hitachi L-7000 system equipped with an L-7400 tunable absorption detector, a Berthold LB 506 B radiometric detector, and either an Xterra C-18 reverse phase column (5  $\mu\text{M}$  4.6 mm  $\times$  150 mm, Waters) (for Re complexes and phosphorylation assays) or a Nucleosil 5 C18 column (5  $\mu\text{M}$  4.6 mm  $\times$  250 mm, Macherey-Nagel) (for  $^{99\text{m}}\text{Tc}$  complexes). HPLC solvents were either H<sub>2</sub>O with 0.1% TFA (solvent A) and MeCN (solvent B) (for Re complexes and phosphorylation assays), TEAP buffer (0.05 M, pH 2.25) (solvent A), and MeOH (solvent B) (for  $^{99\text{m}}\text{Tc}$  complexes) or water (solvent A) and MeOH (solvent B) (for purification of  $^{99\text{m}}\text{Tc}$  complexes) with a flow rate of 1 mL/min. The HPLC system was as follows: 0–15 min, gradient from 95% A to 20% A; 15–20 min, gradient from 20% A to 95% A; 20–30 min, 95% A. Sep-Pak columns (Waters) were washed with methanol and water prior to use. Nuclear magnetic resonance spectra were recorded on a 300 MHz Varian Gemini 2000 spectrometer or a 400 MHz Bruker spectrometer. <sup>1</sup>H and <sup>13</sup>C chemical shifts are reported relative to residual solvent peaks or water as a reference. Radioactivity was measured in a Packard 1900TR  $\beta$ -counter or a Cobra II  $\gamma$ -counter. LC-MS was performed using a Waters Alliance 2795 LC coupled to an ESI-TOF Waters Micromass LCT premier spectrometer for mass detection and a Modulocart QS Uptisphere 3 ODB (4.6 mm  $\times$  150 mm) column. The gradient started with 3% MeCN (+0.1% HCOOH) and 97% H<sub>2</sub>O (+0.1% HCOOH). The system was eluted with this composition for 3 min. The gradient reached 95% MeCN after 15 min, returning to the initial conditions afterward.

Reactions carried out in DMF were worked up using the following general procedure: The reaction mixture was diluted with EtOAc (5  $\times$  reaction volume), washed with water (5  $\times$  reaction volume), and twice with 1 M NaHCO<sub>3</sub> (5  $\times$  reaction volume). The aqueous phases were re-extracted with EtOAc. The organic phases were combined, dried over Na<sub>2</sub>SO<sub>4</sub>, and evaporated under reduced pressure. Unless otherwise stated, the crude product was purified by column chromatography.

**Synthesis of Cysteine Containing Thymidine Derivatives 18, 20, and 21.** **3',5'-Bis-*O*-(*tert*-butyldimethylsilyl)thymidine (1).** Thymidine (1.00 g, 4.13 mmol) and imidazole (1.18 g, 17.34 mmol) were dissolved in DMF (10 mL) and stirred for 5 min at rt. TBDMSCl (1.31 g, 8.67 mmol) was added and the reaction stirred overnight at rt. After workup, the crude product was purified by column chromatography with CH<sub>2</sub>Cl<sub>2</sub> and MeOH (5%) to give **1** as a colorless liquid (1.90 g, 98%). <sup>1</sup>H NMR (CDCl<sub>3</sub>)  $\delta$  8.37 (s, 1H), 7.45 (d, *J* = 0.9 Hz, 1H), 6.30 (m, *J* = 7.9, 5.8 Hz, 1H), 4.38 (m, 1H), 3.91 (m, *J* = 2.5, 2.4, 2.4 Hz, 1H), 3.84 (dd, *J* = 11.4, 2.5 Hz, 1H), 3.74 (dd, *J* = 11.4, 2.4 Hz, 1H), 2.22 (ddd, *J* = 13.1, 5.8, 2.6 Hz, 1H), 2.02–1.89 (m, 1H), 0.90 (s, 9H), 0.87 (s, 9H), 0.09 (s, 6H), 0.05 (s, 6H) ppm. <sup>13</sup>C NMR (CDCl<sub>3</sub>)  $\delta$  164.3, 150.8, 136.2, 111.5, 88.5, 85.5, 73.0, 63.7, 42.1, 19.1, 18.7, 13.2,

26.4, –4.0, –4.7 ppm. MS *m/z* 941.35 [C<sub>44</sub>H<sub>84</sub>N<sub>4</sub>O<sub>10</sub>Si<sub>4</sub>]<sup>+</sup>, 471.08 [C<sub>22</sub>H<sub>42</sub>N<sub>2</sub>O<sub>5</sub>Si<sub>2</sub>]<sup>+</sup>.

**3-(2-Bromoethyl)-3',5'-bis-*O*-(*tert*-butyldimethylsilyl)thymidine (4).** **1** (1.90 g, 4.04 mmol) was dissolved in DMF (10 mL). Cs<sub>2</sub>CO<sub>3</sub> (4.40 g, 12.39 mmol) was added, and the mixture was stirred for 5 min at rt. After addition of 1,2-dibromoethane (7.76 g, 41.28 mmol), the reaction was stirred for 4 h at rt. After workup, the crude product was purified by column chromatography with hexane and EtOAc (20%) to give **4** as a colorless liquid (2.21 g, 95%). <sup>1</sup>H NMR (CDCl<sub>3</sub>)  $\delta$  7.48 (d, *J* = 1.1 Hz, 1H), 6.36 (m, *J* = 7.9, 5.8 Hz, 1H), 4.45–4.29 (m, 3H), 3.95 (m, 1H), 3.87 (dd, *J* = 11.4, 2.6 Hz, 1H), 3.76 (dd, *J* = 11.4, 2.4 Hz, 1H), 3.54 (t, *J* = 7.2 Hz, 2H), 2.30–2.23 (m, 1H), 2.02–1.95 (m, 1H), 1.94 (s, 3H), 0.93 (s, 9H), 0.90 (s, 9H), 0.12 (s, 6H), 0.09 (s, 3H), 0.08 (s, 3H) ppm. <sup>13</sup>C NMR (CDCl<sub>3</sub>)  $\delta$  163.1, 150.7, 133.9, 110.0, 87.9, 85.6, 72.3, 63.0, 42.2, 41.6, 29.5, 25.8, 25.7, 18.4, 18.0, 13.3, –4.6, –4.8, –5.4, –5.4 ppm. MS *m/z* 578.97 [C<sub>24</sub>H<sub>45</sub>BrN<sub>2</sub>O<sub>5</sub>Si<sub>2</sub>]<sup>+</sup>. Anal. (C<sub>24</sub>H<sub>45</sub>BrN<sub>2</sub>O<sub>5</sub>Si<sub>2</sub>) C, H, N.

**3-(5-Bromopentanyl)-3',5'-bis-*O*-(*tert*-butyldimethylsilyl)thymidine (6).** **1** (430 mg, 0.91 mmol) was dissolved in DMF (9 mL). Cs<sub>2</sub>CO<sub>3</sub> (595 mg, 1.83 mmol) was added, and the mixture was stirred for 5 min at rt. After addition of 1,5-dibromopentane (840 mg, 3.65 mmol), the reaction was stirred for 4 h at rt. After workup, the crude product was purified by column chromatography with hexane and EtOAc (10%) to give **6** as a colorless liquid (459 mg, 81%). <sup>1</sup>H NMR (CDCl<sub>3</sub>)  $\delta$  7.42 (d, *J* = 1.1 Hz, 1H), 6.34 (dd, *J* = 5.7, 7.9 Hz, 1H), 4.38 (m, 1H), 3.92 (m, 3H), 3.84 (dd, *J* = 2.7, 11.4 Hz, 1H), 3.74 (dd, *J* = 2.5, 11.4 Hz, 1H), 3.38 (t, *J* = 6.8 Hz, 2H), 2.24 (m, 1H), 1.97 (m, 1H), 1.90 (d, *J* = 1.1 Hz, 3H), 1.88 (m, 2H), 1.62 (m, *J* = 7.8 Hz, 2H), 1.47 (m, *J* = 7.8 Hz, 2H), 0.91 (s, 9H), 0.88 (s, 9H), 0.09 (s, 3H), 0.09 (s, 3H), 0.06 (s, 3H), 0.06 (s, 3H) ppm. <sup>13</sup>C NMR (CDCl<sub>3</sub>)  $\delta$  163.7, 151.1, 133.6, 110.3, 88.0, 85.7, 72.5, 63.2, 41.6, 41.2, 33.8, 32.6, 26.0, 18.7, 18.2, 16.7, 13.5, –4.4, –4.6, –5.1, –5.2 ppm. MS *m/z* 621.07 [C<sub>27</sub>H<sub>51</sub>BrN<sub>2</sub>O<sub>5</sub>Si<sub>2</sub>]<sup>+</sup>.

**3-(10-Bromodecanyl)-3',5'-bis-*O*-(*tert*-butyldimethylsilyl)thymidine (7).** **1** (471 mg, 1.00 mmol) was dissolved in DMF (10 mL). Cs<sub>2</sub>CO<sub>3</sub> (652 mg, 2 mmol) was added and the mixture was stirred for 5 min at rt. After addition of 1,10-dibromodecane (1.20 g, 4.00 mmol), the reaction was stirred for 4 h at rt. After workup, the crude product was purified by column chromatography with hexane and EtOAc (0–9%) to give **7** as a colorless liquid (567 mg, 82%). <sup>1</sup>H NMR (CDCl<sub>3</sub>)  $\delta$  7.43 (s, 1H), 6.37 (m, 1H), 4.40 (m, 1H), 4.12 (q, *J* = 7.1 Hz, 1H), 3.92 (m, 3H), 3.85 (dd, 1H), 3.76 (dd, *J* = 11.4 Hz, 1H), 3.40 (t, *J* = 6.9 Hz, 2H), 2.26 (m, 1H), 1.97 (m, 1H), 1.92 (s, 3H), 1.84 (m, 2H), 1.59 (m, 2H), 1.41 (m, 2H), 1.27 (m, 10H), 0.92 (s, 9H), 0.89 (s, 9H), 0.11 (s, 6H), 0.08 (s, 3H), 0.07 (s, 3H) ppm. <sup>13</sup>C NMR (CDCl<sub>3</sub>)  $\delta$  162.7, 150.4, 134.1, 110.3, 88.1, 85.8, 77.6, 72.5, 70.7, 63.2, 41.7, 30.6, 26.2, 26.0, 25.9, 18.6, 18.2, 13.4, –3.4, –4.4, –4.6, –5.1, –5.2 ppm. MS *m/z* 691.12 [C<sub>32</sub>H<sub>61</sub>BrN<sub>2</sub>O<sub>5</sub>Si<sub>2</sub>]<sup>+</sup>.

**3-{2-[*S*-(*N*-Boc-cysteine methyl ester)]ethyl}-3',5'-bis-*O*-(*tert*-butyldimethylsilyl)thymidine (10).** **4** (2.00 g 3.46 mmol) was dissolved in DMF (35 mL). Cs<sub>2</sub>CO<sub>3</sub> (1.69 g 5.09 mmol) and *N*-Boc-cysteine methyl ester (1.22 g 5.19 mmol) were added, and the mixture was stirred for 2 h at rt. After workup, the crude product was purified by column chromatography with a mixture of hexane and EtOAc (20%) to give **10** (1.90 g, 75%). <sup>1</sup>H NMR (CD<sub>3</sub>OD)  $\delta$  7.58 (d, *J* = 1.0 Hz, 1H), 6.28 (m, *J* = 7.7, 5.9 Hz, 1H), 4.48 (m, *J* = 5.4, 2.5 Hz, 1H), 4.34 (m, 1H), 4.12 (t, *J* = 7.1 Hz, 2H), 3.95 (m, *J* = 8.3, 5.1 Hz, 1H), 3.88 (m, 1H), 3.81 (m, 1H), 3.74 (s, 3H), 3.05 (dd, *J* = 13.6, 5.1 Hz, 1H), 2.90 (dd, *J* = 13.6, 8.3 Hz, 1H), 2.79 (t, *J* = 7.1 Hz, 2H), 2.26 (m, 1H), 2.15 (m, 1H), 1.92 (d, *J* = 1.0 Hz, 3H), 1.44 (s, 9H), 0.95 (s, 9H), 0.93 (s, 9H), 0.14 (s, 6H), 0.13 (s, 6H) ppm. <sup>13</sup>C NMR (CD<sub>3</sub>OD)  $\delta$  165.3, 152.3, 135.9, 110.9, 102.4, 100.8, 89.6, 87.4, 74.1, 64.3, 53.1, 42.2, 34.6, 32.4, 28.7, 26.4, 26.2, 19.3, 18.9, 13.3, –4.5, –4.6, –5.2, –5.2 ppm. MS *m/z* 732.27 [C<sub>33</sub>H<sub>61</sub>N<sub>3</sub>O<sub>9</sub>SSi<sub>2</sub>]<sup>+</sup>.

**3-{5-[*S*-(*N*-Boc-cysteine methyl ester)]pentyl}-3',5'-bis-*O*-(*tert*-butyldimethylsilyl)thymidine (12).** **6** (406 mg 0.66 mmol) was dissolved in DMF (7 mL). Cs<sub>2</sub>CO<sub>3</sub> (326 mg, 1.00 mmol) and

*N*-Boc-cysteine methyl ester (171 mg, 0.73 mmol) were added, and the mixture was stirred for 2 h at rt. After workup, the crude product was purified by column chromatography with a mixture of hexane and EtOAc (12%) to give **12** (394 mg, 78%). <sup>1</sup>H NMR (CDCl<sub>3</sub>) δ 7.41 (d, *J* = 1.1 Hz, 1H), 6.34 (dd, *J* = 5.7, 7.9 Hz, 1H), 5.33 (m, 1H), 4.48 (m, 1H), 4.38 (dt, *J* = 2.6, 5.6 Hz, 1H), 3.91 (m, 3H), 3.84 (dd, *J* = 2.6, 11.3 Hz, 1H), 3.74 (m, 1H), 3.74 (s, 3H), 2.92 (d, *J* = 4.3, 2H), 2.49 (t, *J* = 7.3 Hz, 2H), 2.24 (m, 1H), 1.96 (m, 1H), 1.90 (d, *J* = 1.1 Hz, 3H), 1.60 (m, 4H), 1.42 (s, 9H), 1.37 (m, 2H), 0.91 (s, 9H), 0.87 (s, 9H), 0.09 (s, 3H), 0.09 (s, 3H), 0.06 (s, 3H), 0.05 (s, 3H) ppm. <sup>13</sup>C NMR (CDCl<sub>3</sub>) δ 163.6, 151.0, 133.6, 110.2, 87.9, 85.6, 72.5, 63.2, 60.6, 52.7, 41.6, 41.3, 34.7, 32.8, 29.3, 28.5, 27.3, 26.3, 26.1, 26.0, 21.3, 18.6, 18.2, 14.4, 13.5, -4.4, -4.7, -5.2, -5.2 ppm. MS *m/z* 774.29 [C<sub>36</sub>H<sub>67</sub>N<sub>3</sub>O<sub>9</sub>SSi<sub>2</sub>]H<sup>+</sup>.

**3-[10-(*N*-Boc-cysteine methyl ester)decyl]-3',5'-bis-*O*-(*tert*-butyldimethylsilyl)thymidine (13).** **7** (494 mg, 0.72 mmol) was dissolved in DMF (7 mL). Cs<sub>2</sub>CO<sub>3</sub> (350 mg, 1.07 mmol) and *N*-Boc-cysteine methyl ester (185 mg, 0.79 mmol) were added, and the mixture was stirred for 2 h at rt. After workup, the crude product was purified by column chromatography with a mixture of hexane and EtOAc (12%) to give **13** (565 mg, 93%). <sup>1</sup>H NMR (CDCl<sub>3</sub>) δ 7.43 (d, *J* = 1.1 Hz, 1H), 6.37 (dd, *J* = 5.7, 7.9 Hz, 1H), 5.33 (m, 1H), 4.53 (m, 1H), 4.40 (m, 1H), 3.93 (m, 1H), 3.90 (m, 1H), 3.86 (dd, *J* = 2.6, 11.4 Hz, 1H), 3.76 (s, 3H), 3.76 (dd, *J* = 2.5, 11.4 Hz, 1H), 2.95 (d, *J* = 3.5 Hz, 2H), 2.50 (m, 2H), 2.26 (m, 1H), 1.98 (m, 1H), 1.92 (d, *J* = 1.0 Hz, 3H), 1.55 (m, 4H), 1.45 (s, 9H), 1.31 (m, 6H), 1.26 (m, 6H), 0.93 (s, 9H), 0.89 (s, 9H), 0.11 (s, 3H), 0.11 (s, 3H), 0.08 (s, 3H), 0.07 (s, 3H) ppm. <sup>13</sup>C NMR (CDCl<sub>3</sub>) δ 171.9, 163.4, 151.1, 133.5, 110.2, 88.0, 85.6, 72.5, 63.3, 52.7, 41.8, 34.7, 29.7, 29.3, 28.6, 27.2, 25.9, 22.9, 18.2, 14.3, 13.5, -4.4, -4.6, -5.2, -5.3 ppm. MS *m/z* 844.41 [C<sub>41</sub>H<sub>77</sub>N<sub>3</sub>O<sub>9</sub>SSi<sub>2</sub>]H<sup>+</sup>.

**3-[2-(*S*-Cysteinyl)ethyl]thymidine (18).** **10** (731 mg, 1.00 mmol) was dissolved in MeOH (50 mL). Concentrated HCl (1 mL) was added, and the mixture was stirred for 4 h at rt. The solvent volume was reduced to ca. 15 mL and diluted with water (10 mL). The pH was increased to 12 with 5 M NaOH and stirred at rt for 2 h. The mixture was neutralized by addition of 1 M HCl, concentrated under reduced pressure, and purified by solid phase extraction using a Sep-Pak column. The fractions containing the product were evaporated under vacuum to give **18** (241 mg, 62%). <sup>1</sup>H NMR (CD<sub>3</sub>OD) δ 7.88 (d, *J* = 0.8 Hz, 1H), 6.31 (t, *J* = 6.7 Hz, 1H), 4.41 (m, 1H), 4.28 (m, *J* = 7.8, 4.3 Hz, 1H), 4.17 (m, 2H), 3.93 (m, *J* = 3.3 Hz, 1H), 3.81 (dd, *J* = 12.0, 3.3 Hz, 1H), 3.74 (dd, *J* = 12.0, 3.8 Hz, 1H), 3.28 (dd, *J* = 14.8, 4.4 Hz, 1H), 3.10 (dd, *J* = 14.8, 8.0 Hz, 1H), 2.88 (m, 2H), 2.28 (m, 1H), 2.20 (m, 1H), 1.92 (d, *J* = 0.8 Hz, 3H) ppm. <sup>13</sup>C NMR (CD<sub>3</sub>OD) δ 170.5, 165.5, 152.5, 137.0, 110.9, 89.1, 87.3, 72.3, 62.9, 53.5, 41.4, 41.3, 32.9, 30.5, 13.3 ppm. MS *m/z* 389.91 [C<sub>15</sub>H<sub>23</sub>N<sub>3</sub>O<sub>7</sub>S]H<sup>+</sup>. Anal. (C<sub>15</sub>H<sub>23</sub>N<sub>3</sub>O<sub>7</sub>S) C, H, N.

**3-[5-(*S*-Cysteinyl)pentyl]thymidine (20).** **12** (375 mg, 0.48 mmol) was dissolved in MeOH (25 mL). Concentrated HCl (1 mL) was added, and the mixture was stirred for 4 h at rt. The solvent volume was reduced to ca. 10 mL and diluted with water (7 mL). The pH was increased to 12 with 5 M NaOH and stirred at rt for 2 h. The mixture was neutralized by addition of 1 M HCl, concentrated under reduced pressure, and purified by solid phase extraction using a Sep-Pak column. The fractions containing the product were evaporated under vacuum to give **20** (168 mg, 80%). <sup>1</sup>H NMR (D<sub>2</sub>O) δ 7.69 (s, 1H), 6.35 (t, *J* = 6.6 Hz, 1H), 4.50 (m, 1H), 4.07 (m, *J* = 3.9 Hz, 1H), 3.93 (m, 4H), 3.81 (dd, *J* = 5.0, 12.4 Hz, 1H), 3.14 (dd, *J* = 4.0, 14.6 Hz, 1H), 3.03 (dd, 1H, *J* = 7.6, 14.6), 2.66 (t, *J* = 7.1 Hz, 2H), 2.41 (m, 2H), 1.67 (m, 4H), 1.46 (m, 2H) ppm. <sup>13</sup>C NMR (D<sub>2</sub>O) δ 174.0, 166.2, 152.3, 136.0, 111.3, 87.1, 86.5, 70.9, 61.8, 54.3, 42.0, 39.2, 33.0, 31.8, 28.8, 26.9, 25.7, 12.9 ppm. MS *m/z* 431.89 [C<sub>18</sub>H<sub>29</sub>N<sub>3</sub>O<sub>7</sub>S]H<sup>+</sup>.

**3-[10-(*S*-Cysteinyl)decyl]thymidine (21).** **13** (524 mg, 0.62 mmol) was dissolved in MeOH (30 mL). Concentrated HCl (1.2 mL) was added, and the mixture was stirred for 4 h at rt. The solvent volume was reduced to ca. 10 mL and diluted with water (5 mL). The pH was increased to 12 with 5 M NaOH and stirred at rt for 2 h. The mixture was neutralized by addition of 1 M HCl,

concentrated under reduced pressure, and purified by solid phase extraction using a Sep-Pak column. The fractions containing the product were evaporated under vacuum to give **21** (243 mg, 78%). <sup>1</sup>H NMR (CD<sub>3</sub>OD) δ 7.83 (s, 1H), 6.31 (t, *J* = 6.6 Hz, 1H), 4.40 (m, 1H), 3.91 (m, 3H), 3.81 (dd, *J* = 12.0 Hz, 1H), 3.74 (dd, 1H), 3.66 (dd, *J* = 5.3 Hz, 1H), 3.16 (dd, *J* = 14.7 Hz, 1H), 2.88 (dd, *J* = 9.0, 14.7 Hz, 1H), 2.61 (t, *J* = 7.4 Hz, 2H), 2.27 (m, 1H), 2.22 (m, 1H), 1.91 (s, 3H), 1.60 (m, 4H), 1.41 (m, 2H), 1.31 (m, 10H) ppm. <sup>13</sup>C NMR (CD<sub>3</sub>OD) δ 165.4, 152.5, 136.5, 110.8, 89.0, 87.3, 72.2, 62.9, 42.4, 41.5, 34.2, 32.9, 30.7, 30.4, 29.9, 28.6, 28.0, 13.4 ppm. MS *m/z* 502.02 [C<sub>23</sub>H<sub>39</sub>N<sub>3</sub>O<sub>7</sub>S]H<sup>+</sup>.

**Synthesis of Rhenium Complexes.** Tricarbonyl rhenium complexes (**22a–27a**) were synthesized according to the following general procedure: One equivalent of thymidine containing ligand was dissolved in a mixture of MeOH and water (1:1, compounds **16–20**, 3:1 compound **21**) to form a 0.1 M solution. The pH was adjusted to 7 with NaOH/HCl before addition of one equivalent of [ReBr<sub>3</sub>(CO)<sub>3</sub>][NET<sub>4</sub>]<sub>2</sub>. The reaction was stirred at 50 °C for 2 h and followed by HPLC. The solvents were removed under vacuum, and the residue was purified by solid phase extraction using a Sep-Pak column with a water–MeOH gradient to give the Re(CO)<sub>3</sub> complex as a white powder. Analytical data for the rhenium complexes **22a–27a** can be found in the Supporting Information.

**Synthesis of Technetium Complexes.** The technetium-99m complexes, **22b–27b**, were synthesized according to the following general procedure: A solution of [<sup>99m</sup>Tc(CO)<sub>3</sub>(H<sub>2</sub>O)<sub>3</sub>]<sup>+</sup> (50 μL; ~500 MBq mL<sup>-1</sup>) was added to a 10<sup>-3</sup> M solution of the relevant ligand (50 μL) diluted with PBS (400 μL; pH 7.4) to give a final ligand concentration of 10<sup>-4</sup> M. The reaction mixtures were heated for 45 min at 95 °C. The radioactive product was separated from unlabeled ligand by HPLC. The complexes were characterized by comparison of their HPLC retention times (*γ*-trace) with those of their rhenium analogues **22a–27a** (UV-trace).

**Phosphorylation Transfer Assays.** Thymidine analogues **22–27** were assayed at 37 °C for 1 h in 200 μL of a mixture containing 112.3 μL of water, 10 μL of 1 M HEPES buffer (pH 7.5), 0.2 μL of 1 M DTT, 0.5 μL of 1 M MgCl<sub>2</sub>, 2 μL of 100 mM ATP, 5 μL of hTK1 (~0.5 mg/mL), 20 μL of a 10 mM solution of **22a–27a**, and 50 μL of an aqueous solution of **22b–27b** (~100 kBq). The reaction mixtures were quenched by addition of 800 μL of 5 mM EDTA solution and analyzed by HPLC.

Thymidine, 3-(2-propyn-1-yl)thymidine, and thymidine analogues **22a–27a** were assayed at 25 °C for 15 min in 200 μL of a mixture containing 155.38 μL of water, 10 μL of 1 M HEPES buffer (pH 7.5), 0.2 μL of 1 M DTT, 0.42 μL of 100 mM PEP, 0.5 μL of 1 M MgCl<sub>2</sub>, 7.2 μL of 5 mM NADH, 2 μL of 100 mM ATP, 0.6 μL of pyruvate kinase (1350 U/mL), 0.7 μL of lactate dehydrogenase (1420 U/mL), 5 μL of hTK1 (~0.5 mg/mL), and 20 μL of a 10 mM solution of thymidine, 3-(2-propyn-1-yl)thymidine, or the thymidine analogues **22a–26a**. For complex **27a**, a 1 mM solution was used to avoid precipitation of the complex over the course of the reaction.

For each substrate, the linear decrease in UV absorption at 340 nm was measured from 0 to 15 min. The gradients of the regression lines between 6 and 12 min were compared to thymidine, the phosphorylation of which was assumed to be 100% (see Supporting Information for more information).

**Octanol/Water Partition Coefficient Studies.** Octanol/water partition coefficients were determined for the 99m-technetium labeled compounds **22b–27b** by measuring the distribution of the radiolabeled compound between 1-octanol and PBS (pH = 7.4). Six kBq of radiolabeled compound in saline was added to a vial containing 0.5 mL each of 1-octanol and PBS. After vortexing for 1 min, the vial was centrifuged for 5 min to ensure complete separation of the layers. The technetium-99m activity in 200 μL of each layer was measured using a Cobra II *γ*-counter. Counts per unit weight of sample were calculated, and log *P* values were determined using the formula log<sub>10</sub> *P* = log<sub>10</sub>(counts in 1 g of octanol/counts in 1 g of water) as described by Pillarsety et al.<sup>39</sup>

**Cell Cultures.** SKNMC human neuroblastoma cells (ATCC, Manassas, VA) were grown in MEM medium containing 10% FCS, 0.2% nonessential amino acids, 1% sodium pyruvate 100 mM, 100 IU/mL penicillin, 100  $\mu\text{g}/\text{mL}$  streptomycin, and 0.25  $\mu\text{g}/\text{mL}$  amphotericin B. Cells were grown in a 5%  $\text{CO}_2$ -humidified atmosphere at 37 °C. The cells were detached with trypsin/PBS for 2–5 min, resuspended in the culture media, and subcultured weekly.

**In Vitro Uptake Studies.** Cells (70–90% confluence) suspended in 2 mL of culture medium were seeded into six-well plates (~1000000 cells/well). The plates were incubated for 16 h in a 5%  $\text{CO}_2$ -humidified atmosphere at 37 °C. The medium was removed and replaced by fresh culture medium containing ~6 kBq of technetium complex (or 111 kBq of [ $^3\text{H}$ ]thymidine). After 2 h, the medium was removed and the cells washed with  $1 \times 500 \mu\text{L}$  cold PBS (4 °C). Cells were detached by addition of  $2 \times 500 \mu\text{L}$  1 M NaOH. The radioactivity in the collected cells and the medium was counted in a  $\gamma$ -counter (or  $\beta$ -counter for [ $^3\text{H}$ ]thymidine). The protein content was determined spectrophotometrically using a Micro BCA protein assay reagent kit (Pierce, Socochim). The data were expressed as a ratio of the activity of the protein to the activity of the medium (cpm/mg cells)/(cpm/mL medium) to give %ID/(mg/mL), where ID is injected dose. Each experiment was performed in triplicate.

**Computational Studies.** The initial coordinates of the hTK1 homology model were constructed with the Modeler package using *C. acetobutylicum* thymidine kinase (1XX6) as a template for the lasso-like loop region, while the structure of human thymidine kinase 1 (1W4R) was used for the rest of the model.<sup>40</sup> The homology model was solvated with the utility genbox of the GROMACS package and parametrized using the GROMOS 53A6 force field. The parametrization of the zinc region was carried out using GROMOS 53A6 parameters and ab initio calculations on the B3LYP/6-31G\* level with the GAMESS US package. The homology model was minimized with the GROMOS 53A6 force-field until the gradient reached  $1 \text{ J mol}^{-1} \text{ nm}^{-1}$ . Force field parameters of thymidine and compounds **24a**, **26a**, and **27a** were derived from the topologies of deoxythymidine, amino acids, and a heme–CO complex using the GROMOS 53A6 force field (the topology of **26a** is available as supporting material).<sup>44</sup> Charges were customized using wave functions calculated for fragments of the compounds investigated using the HF/MINI (metal-containing) or HF/6-31G\* level of theory.

All simulations were carried out using GROMACS 3.1.1.<sup>45</sup> Individual compounds were superimposed on to dTTP as it is found in the crystal structure by using the match utility of the software Moloc.<sup>46</sup> Energy minimization with a tolerance of  $1 \text{ J mol}^{-1} \text{ nm}^{-1}$  was carried out using the steepest descent minimizer. For MD simulations, the system was coupled to a temperature bath using Berendsen's method. Long-range electrostatic interactions were handled using the PME method. The electrostatic potential cutoff was set to 0.9 nm and the Van der Waals potential cutoff to 1 nm. All bonds were constrained using the LINCS algorithm. The first MD simulation was performed with restrained positions of non-hydrogen protein atoms over 20 ps with a time-step of 2 fs to equilibrate the water molecules inside the protein. Subsequent MD simulations were performed over 1 ns with a time-step of 2 fs without any positional restraints.

**Acknowledgment.** We thank Prof. L. Scapozza and Anja Stoffel (University of Geneva, Switzerland) for kindly providing hTK1 and for helpful discussions. This work was supported by Mallinckrodt-Tyco.

**Supporting Information Available:** Experimental procedures and characterization data for the synthesis of compounds **1–21**, **22a–27a**, and 3-(2-Propyn-1-yl)thymidine, analytical data for target compounds **16–21** and **22a–27a**, further analysis of the phosphorylation experiments, and additional information regarding the

computational studies. This material is available free of charge via the Internet at <http://pubs.acs.org>.

## References

- (1) Eriksson, S.; Munch-Petersen, B.; Johansson, K.; Eklund, H. Structure and function of cellular deoxyribonucleoside kinases. *Cell. Mol. Life Sci.* **2002**, *59*, 1327–1346.
- (2) Sherley, J. L.; Kelly, T. J. Regulation of Human Thymidine Kinase During the Cell-Cycle. *J. Biol. Chem.* **1988**, *263*, 8350–8358.
- (3) Hengstschlager, M.; Knofler, M.; Mullner, E. W.; Ogris, E.; Wintersberger, E.; Wawra, E. Different Regulation of Thymidine Kinase During the Cell-Cycle of Normal Versus DNA Tumor Virus-Transformed Coils. *J. Biol. Chem.* **1994**, *269*, 13836–13842.
- (4) Hengstschlager, M.; Pusch, O.; Hengstschlager-Ottmad, E.; Ambros, P. F.; Bernaschek, G.; Wawra, E. Loss of the p16/MTS1 tumor suppressor gene causes E2F-mediated deregulation of essential enzymes of the DNA precursor metabolism. *DNA Cell Biol.* **1996**, *15*, 41–51.
- (5) Munchpetersen, B.; Tyrsted, G.; Cloos, L.; Beck, R. A.; Eger, K. Different Affinity of the 2 Forms of Human Cytosolic Thymidine Kinase Towards Pyrimidine Analogs. *Biochim. Biophys. Acta, Protein Struct. Mol. Enzymol.* **1995**, *1250*, 158–162.
- (6) O'Neill, K. L.; Hoper, M.; Odlingmsee, G. W. Can Thymidine Kinase Levels in Breast Tumors Predict Disease Recurrence? *J. Natl. Cancer Inst.* **1992**, *84*, 1825–1828.
- (7) Yusa, T.; Yamaguchi, Y.; Ohwada, H.; Hayashi, Y.; Kuroiwa, N.; Morita, T.; Asanagi, M.; Moriyama, Y.; Fujimura, S. Activity of the Cytosolic Isozyme of Thymidine Kinase in Human Primary Lung-Tumors with Reference to Malignancy. *Cancer Res.* **1988**, *48*, 5001–5006.
- (8) Buchmann, I.; Vogg, A. T. J.; Glatting, G.; Schultheiss, S.; Moller, P.; Leithausser, F.; Schulte, M.; Gfrorer, W.; Kotzerke, J.; Reske, S. N. F-18 5-fluoro-2-deoxyuridine-PET for imaging of malignant tumors and for measuring tissue proliferation. *Cancer Biother. Radiopharm.* **2003**, *18*, 327–337.
- (9) Gardelle, O.; Roelcke, U.; Vontobel, P.; Crompton, N. E. A.; Guenther, I.; Blauenstein, P.; Schubiger, A. P.; Blattmann, H.; Ryser, J. E.; Leenders, K. L.; Kaser-Hotz, B. [ $^{76}\text{Br}$ ]Bromodeoxyuridine PET in tumor-bearing animals. *Nucl. Med. Biol.* **2001**, *28*, 51–57.
- (10) Al-Madhoun, A. S.; Johnsamuel, J.; Barth, R. F.; Tjarks, W.; Eriksson, S. Evaluation of human thymidine kinase 1 substrates as new candidates for boron neutron capture therapy. *Cancer Res.* **2004**, *64*, 6280–6286.
- (11) Al-Madhoun, A. S.; Johnsamuel, J.; Yan, J. H.; Ji, W. H.; Wang, J. H.; Zhuo, J. C.; Lunato, A. J.; Woollard, J. E.; Hawk, A. E.; Cosquer, G. Y.; Blue, T. E.; Eriksson, S.; Tjarks, W. Synthesis of a small library of 3-(Carboranylalkyl)thymidines and their biological evaluation as substrates for human thymidine kinases 1 and 2. *J. Med. Chem.* **2002**, *45*, 4018–4028.
- (12) Barth, R. F.; Yang, W. L.; Al-Madhoun, A. S.; Johnsamuel, J.; Byun, Y.; Chandra, S.; Smith, D. R.; Tjarks, W.; Eriksson, S. Boron-containing nucleosides as potential delivery agents for neutron capture therapy of brain tumors. *Cancer Res.* **2004**, *64*, 6287–6295.
- (13) Byun, Y.; Yan, J.; Al-Madhoun, A. S.; Johnsamuel, J.; Yang, W. L.; Barth, R. F.; Staffan, E.; Tjarks, W. The synthesis and biochemical evaluation of thymidine analogues substituted with nido carborane at the N-3 position. *Appl. Radiat. Isot.* **2004**, *61*, 1125–1130.
- (14) Johnsamuel, J.; Lakhi, N.; Al-Madhoun, A. S.; Byun, Y.; Yan, J. H.; Eriksson, S.; Tjarks, W. Synthesis of ethyleneoxide modified 3-carboranyl thymidine analogues and evaluation of their biochemical, physicochemical, and structural properties. *Bioorg. Med. Chem.* **2004**, *12*, 4769–4781.
- (15) Yan, J. H.; Naeslund, C.; Al-Madhoun, A. S.; Wang, J. H.; Ji, W. H.; Cosquer, G. Y.; Johnsamuel, J.; Sjoberg, S.; Eriksson, S.; Tjarks, W. Synthesis and biological evaluation of 3'-carboranyl thymidine analogues. *Bioorg. Med. Chem. Lett.* **2002**, *12*, 2209–2212.
- (16) Schmid, M.; Neumaier, B.; Vogg, A. T. J.; Wezasek, K.; Friesen, C.; Mottaghy, F. M.; Buck, A. K.; Reske, S. N. Synthesis and evaluation of a radiometal-labeled macrocyclic chelator-derivatised thymidine analog. *Nucl. Med. Biol.* **2006**, *33*, 359–366.
- (17) Celen, S.; De Groot, T. J.; Balzarini, J.; Vunckx, K.; Terwinghe, C.; Vermaelen, P.; Van Berckelaer, L.; Vanbilloen, H.; Nuyts, J.; Mortelmans, L.; Verbruggen, A.; Bormans, G. Synthesis and evaluation of a Tc-99m-MAMA-propyl-thymidine complex as a potential probe for in vivo visualization of tumor cell proliferation with SPECT. *Nucl. Med. Biol.* **2007**, *34*, 283–291.
- (18) Alberto, R.; Ortner, K.; Wheatley, N.; Schibli, R.; Schubiger, A. P. Synthesis and Properties of Boranocarbonate: a convenient in situ CO source for the aqueous preparation of [ $^{99\text{m}}\text{Tc}(\text{H}_2\text{O})_3(\text{CO})_3$ ] $^+$ . *J. Am. Chem. Soc.* **2001**, *123*, 3135–3136.

- (19) Alberto, R.; Schibli, R.; Egli, A.; Schubiger, A. P.; Abram, U.; Kaden, T. A. A novel organometallic aqua complex of technetium for the labeling of biomolecules: synthesis of  $[\text{}^{99\text{m}}\text{Tc}(\text{OH})_2)_3(\text{CO})_3]^+$  from  $[\text{}^{99\text{m}}\text{TcO}_4]^-$  in aqueous solution and its reaction with a bifunctional ligand. *J. Am. Chem. Soc.* **1998**, *120*, 7987–7988.
- (20) Schibli, R.; Schubiger, P. A. Current use and future potential of organometallic radiopharmaceuticals. *Eur. J. Nucl. Med. Mol. Imaging* **2002**, *29*, 1529–1542.
- (21) Schibli, R.; Netter, M.; Scapozza, L.; Birringer, M.; Schelling, P.; Dumas, C.; Schoch, J.; Schubiger, P. A. First organometallic inhibitors for human thymidine kinase: synthesis and in vitro evaluation of rhenium(I)- and technetium(I)-tricarboxyl complexes of thymidine. *J. Organomet. Chem.* **2003**, *668*, 67–74.
- (22) Desbouis, D.; Schubiger, A. P.; Schibli, R. Synthesis of tricarboxyl rhenium and technetium complexes of a 5'-carboxamide 5-ethyl-2'-deoxyuridine for selective inhibition of herpes simplex virus thymidine kinase 1. *J. Organomet. Chem.* **2007**, *692*, 1340–1347.
- (23) Stichelberger, M.; Desbouis, D.; Spiwok, V.; Scapozza, L.; Schubiger, A. P.; Schibli, R. Synthesis, in vitro and in silico assessment of organometallic rhenium(I) and technetium(I) thymidine complexes. *J. Organomet. Chem.* **2007**, *692*, 1255–1264.
- (24) Birringer, M. S.; Claus, M. T.; Folkers, G.; Kloer, D. P.; Schulz, G. E.; Scapozza, L. Structure of a type II thymidine kinase with bound dTTP. *FEBS Lett.* **2005**, *579*, 1376–1382.
- (25) Welin, M.; Kosinska, U.; Mikkelsen, N. E.; Carnrot, C.; Zhu, C. Y.; Wang, L. Y.; Eriksson, S.; Munch-Petersen, B.; Eklund, H. Structures of thymidine kinase 1 of human and mycoplasmic origin. *Proc. Natl. Acad. Sci. U.S.A.* **2004**, *101*, 17970–17975.
- (26) Wild, K.; Bohner, T.; Aubry, A.; Folkers, G.; Schulz, G. E. The 3-Dimensional Structure of Thymidine Kinase from Herpes-Simplex Virus Type-1. *FEBS Lett.* **1995**, *368*, 289–292.
- (27) Byun, Y.; Thirumamagal, B. T. S.; Yang, W.; Eriksson, S.; Barth, R. F.; Tjarks, W. Preparation and Biological Evaluation of 10B-Enriched 3-[5-{2-(2,3-Dihydroxyprop-1-yl)-o-carboran-1-yl}pentan-1-yl]thymidine (N5-2OH), a New Boron Delivery Agent for Boron Neutron Capture Therapy of Brain Tumors. *J. Med. Chem.* **2006**, *49*, 5513–5523.
- (28) Byun, Y.; Yan, J. H.; Al-Madhoun, A. S.; Johnsamuel, J.; Yang, W. L.; Barth, R. F.; Eriksson, S.; Tjarks, W. Synthesis and biological evaluation of neutral and zwitterionic 3-carboranyl thymidine analogues for boron neutron capture therapy. *J. Med. Chem.* **2005**, *48*, 1188–1198.
- (29) Lunato, A. J.; Wang, J. H.; Woollard, J. E.; Anisuzzaman, A. K. M.; Ji, W. H.; Rong, F. G.; Ikeda, S.; Soloway, A. H.; Eriksson, S.; Ives, D. H.; Blue, T. E.; Tjarks, W. Synthesis of 5-(carboranylalkylmercapto)-2'-deoxyuridines and 3-(carboranylalkyl)thymidines and their evaluation as substrates for human thymidine kinases 1 and 2. *J. Med. Chem.* **1999**, *42*, 3378–3389.
- (30) Struthers, H.; Spingler, B.; Mindt, T. L.; Schibli, R. "Click-to-Chelate": Design and Incorporation of Triazole-Containing Metal-Chelating Systems into Biomolecules of Diagnostic and Therapeutic Interest. *Chem.—Eur. J.* **2008**, *14*, 6173–6183.
- (31) Banerjee, S. R.; Levadala, M. K.; Lazarova, N.; Wei, L. H.; Valliant, J. F.; Stephenson, K. A.; Babich, J. W.; Maresca, K. P.; Zubieta, J. Bifunctional single amino acid chelates for labeling of biomolecules with the  $\{\text{Tc}(\text{CO})_3\}^+$  and  $\{\text{Re}(\text{CO})_3\}^+$  cores. Crystal and molecular structures of  $\text{ReBr}(\text{CO})_3(\text{H}_2\text{NCH}_2\text{C}_5\text{H}_4\text{N})$ ,  $\text{Re}(\text{CO})_3\{(\text{C}_5\text{H}_4\text{NCH}_2)_2\text{NH}\}$  Br,  $\text{Re}(\text{CO})_3\{(\text{C}_5\text{H}_4\text{NCH}_2)_2\text{NCH}_2\text{CO}_2\text{H}\}$  Br,  $\text{Re}(\text{CO})_3\{X(Y)\text{NCH}_2\text{CO}_2\text{CH}_2\text{CH}_3\}$  Br (X = Y = 2-pyridylmethyl; X = 2-pyridylmethyl, Y = 2-(1-methylimidazolyl)methyl; X = Y = 2-(1-methylimidazolyl)methyl),  $\text{ReBr}(\text{CO})_3\{(\text{C}_5\text{H}_4\text{NCH}_2)\text{NH}(\text{CH}_2\text{C}_4\text{H}_3\text{S})\}$ , and  $\text{Re}(\text{CO})_3\{(\text{C}_5\text{H}_4\text{NCH}_2)\text{N}(\text{CH}_2\text{C}_4\text{H}_3\text{S})(\text{CH}_2\text{CO}_2)\}$ . *Inorg. Chem.* **2002**, *41*, 6417–6425.
- (32) Mundwiler, S.; Kundig, M.; Ortner, K.; Alberto, R. A new [2 + 1] mixed ligand concept based on  $[\text{}^{99\text{m}}\text{Tc}(\text{OH})_2)_3(\text{CO})_3]^+$ : a basic study. *J. Chem. Soc., Dalton Trans.* **2004**, 1320–1328.
- (33) Schibli, R.; La Bella, R.; Alberto, R.; Garcia-Garayoa, E.; Ortner, K.; Abram, U.; Schubiger, P. A. Influence of the denticity of ligand systems on the in vitro and in vivo behavior of Tc-99m(I)-tricarboxyl complexes: a hint for the future functionalization of biomolecules. *Bioconjugate Chem.* **2000**, *11*, 345–351.
- (34) van Staveren, D. R.; Benny, P. D.; Waibel, R.; Kurz, P.; Pak, J. K.; Alberto, R. S-functionalized cysteine: Powerful ligands for the labelling of bioactive molecules with triaquatrichlorotechnetium  $[\text{}^{99\text{m}}\text{Tc}(\text{OH})_2)_3(\text{CO})_3]^+$ . *Helv. Chim. Acta* **2005**, *88*, 447–460.
- (35) Wei, L. H.; Babich, J.; Zubieta, J. Bifunctional chelates with mixed aromatic and aliphatic amine donors for labeling of biomolecules with the  $\{\text{Tc}(\text{CO})_3\}^+$  and  $\{\text{Re}(\text{CO})_3\}^+$  cores. *Inorg. Chim. Acta* **2005**, *358*, 3691–3700.
- (36) Ogilvie, K. K. *tert*-Butyldimethylsilyl Group as a Protecting Group in Deoxynucleosides. *Can. J. Chem.* **1973**, *51*, 3799–3807.
- (37) Schibli, R.; Alberto, R.; Abram, U.; Abram, S.; Egli, A.; Schubiger, P. A.; Kaden, T. A. Structural and Tc-99 NMR investigations of complexes with  $\text{fac-}[\text{Tc}(\text{CO})_3]^+$  moieties and macrocyclic thioethers of various ring sizes: synthesis and X-ray structure of the complexes  $\text{fac-}[\text{Tc}(\text{9-ane-S-3})(\text{CO})_3]\text{Br}$ ,  $\text{fac-}[\text{Tc}_2(\text{tosylate})_2(18\text{-ane-S-6})(\text{CO})_6]$ , and  $\text{fac-}[\text{Tc}_2(20\text{-ane-S-6-OH})(\text{CO})_6][\text{tosylate}]_2$ . *Inorg. Chem.* **1998**, *37*, 3509–3516.
- (38) Kornberg, A.; Pricer, W. E. Enzymatic phosphorylation of adenosine and 2,6-diaminopurine riboside. *J. Biol. Chem.* **1951**, *193*, 481–495.
- (39) Pillarsetty, N.; Cai, S. D.; Ageyeva, L.; Finn, R. D.; Blasberg, R. G. Synthesis and evaluation of [ $^{18}\text{F}$ ] labeled pyrimidine nucleosides for positron emission tomography imaging of herpes simplex virus 1 thymidine kinase gene expression. *J. Med. Chem.* **2006**, *49*, 5377–5381.
- (40) Narayanasamy, S.; Thirumamagal, B. T. S.; Johnsamuel, J.; Byun, Y.; Al-Madhoun, A. S.; Usova, E.; Cosquer, G. Y.; Yan, J. H.; Bandyopadhyaya, A. K.; Tiwari, R.; Eriksson, S.; Tjarks, W. Hydrophilically enhanced 3-carboranyl thymidine analogues (3CTAs) for boron neutron capture therapy (BNCT) of cancer. *Bioorg. Med. Chem.* **2006**, *14*, 6886–6899.
- (41) Kosinska, U.; Carnrot, C.; Sandrini, M. P. B.; Clausen, A. R.; Wang, L. Y.; Piskur, J.; Eriksson, S.; Eklund, H. Structural studies of thymidine kinases from *Bacillus anthracis* and *Bacillus cereus* provide insights into quaternary structure and conformational changes upon substrate binding. *FEBS J.* **2007**, *274*, 727–737.
- (42) Segura-Pena, D.; Lichter, J.; Trani, M.; Konrad, M.; Lavie, A.; Lutz, S. Quaternary structure change as a mechanism for the regulation of thymidine kinase 1-like enzymes. *Structure* **2007**, *15*, 1555–1566.
- (43) Alberto, R.; Egli, A.; Abram, U.; Hegetschweiler, K.; Gramlich, V.; Schubiger, P. A. Synthesis and Reactivity of  $[\text{NEt}_4][\text{ReBr}_3(\text{CO})_3]$ . Formation and Structural Characterization of the Clusters  $[\text{NEt}_4][\text{Re}(\mu\text{-OH})(\mu\text{-OH})_3(\text{CO})_3]$  and  $[\text{NEt}_4][\text{Re}_2(\mu\text{-OH})_3(\text{CO})_6]$  by Alkaline Titration. *J. Chem. Soc., Dalton Trans.* **1994**, 2815–2820.
- (44) Oostenbrink, C.; Villa, A.; Mark, A. E.; Van Gunsteren, W. F. A biomolecular force field based on the free enthalpy of hydration and solvation: the GROMOS force-field parameter sets 53A5 and 53A6. *J. Comput. Chem.* **2004**, *25*, 1656–1676.
- (45) Lindahl, E.; Hess, B.; van der Spoel, D. GROMACS 3.0: a package for molecular simulation and trajectory analysis. *J. Mol. Modeling* **2001**, *7*, 306–317.
- (46) Gerber, P. R.; Muller, K. Mab, a Generally Applicable Molecular Force Field for Structure Modeling in Medicinal Chemistry. *J. Comput.-Aided Mol. Des.* **1995**, *9*, 251–268.

JM800530P